

Precision and postscission charged particle emissions from the $^{19}\text{F} + ^{159}\text{Tb}$ reaction

H. Ikezoe, Y. Nagame, I. Nishinaka, Y. Sugiyama, Y. Tomita, K. Ideno,
S. Hamada, N. Shikazono, and A. Iwamoto

Advanced Science Research Center, Japan Atomic Energy Research Institute, Tokai-mura, Ibaraki-ken 319-11, Japan

T. Ohtsuki

Laboratory of Nuclear Science, Tohoku University, Sendai-shi, Miyagi-ken 982, Japan

(Received 13 September 1993)

Precision and postscission multiplicities of protons and α particles are measured in the $^{19}\text{F} + ^{159}\text{Tb}$ reaction. The observed precision multiplicities are enhanced compared to statistical model predictions and the presaddle delay time of around 0.5×10^{-20} sec is needed to reproduce both precision proton and α particle multiplicities. This value is too small to account for the precision neutron data measured by Newton *et al.*, suggesting a long saddle-to-scission time. The measured postscission multiplicities of protons and α particles indicate that fission fragments are rather colder than the statistical model predictions, but slightly hotter than the estimation from the observed precision and postscission neutron multiplicities.

PACS number(s): 24.75.+i

I. INTRODUCTION

Time scales in the fission process are one of the most important quantities in studying nuclear viscosity. Since fission is a dynamical motion of a viscous nucleus, a finite time is needed for a fissioning nucleus to reach a scission configuration. During this time scale, which is called a fission delay time, neutrons, protons, and α particles can be emitted. Hinde *et al.* [1] have determined the fission delay time of $(3.5 \pm 1.5) \times 10^{-20}$ from an excess of measured precision neutrons relative to statistical-model predictions. This long time scale indicates that fission is characterized as a overdamped motion [2–9]. In connection to this, we have previously reported measurements of precision multiplicities of protons and α particles from the compound nuclei ^{200}Pb , ^{213}Fr , ^{216}Ra , ^{225}Np , and ^{236}Cm [10]. Contrary to the expectation, the observed precision multiplicities of charged particles agreed rather well with statistical-model predictions without taking into account the fission delay time. In order to explain both results consistently, we have concluded [10] that charged particles, especially α particles, are predominantly emitted from highly excited nucleus at an initial stage of the fission process before saddle, while neutrons may be emitted from the saddle-to-scission region as well as the presaddle region. Thus the disagreement of the neutron and charged particle results was ascribed to additional emissions of neutrons from the saddle-to-scission region. This conclusion is qualitatively similar to the one obtained by Lestone *et al.* [11]; that is, it is not possible to obtain fits to neutron, proton, and α particle multiplicities using only a presaddle delay to fission. A relatively short presaddle delay ($\leq 1.0 \times 10^{-20}$ sec) and a long saddle-to-scission time of 5×10^{-20} sec are needed to obtain good fits to those multiplicities in their analysis.

In the present paper, we report the measurement of precision and postscission proton and α particle multiplicities in the $^{19}\text{F} + ^{159}\text{Tb}$ reaction where the compound

nucleus ^{178}W is formed. The emphasis is that the precision charged particle multiplicities in the ^{178}W are so sensitive to the presaddle delay time that the presaddle delay time is definitely determined. In addition, according to the rotating liquid drop model [12], the nucleus ^{178}W whose fissility x is 0.637 has a saddle point shape close to its scission configuration compared to the heavier nuclei previously studied ($x = 0.7 - 0.82$). This means that the saddle-to-scission path length is rather shorter than the ones for the heavy nuclei. On the other hand, it has been reported that the fission delay times deduced from the measured precision and postscission neutron multiplicities are rather independent from the fissility of nucleus [6]. We examined this issue by measuring the postscission charged particle multiplicities which depend on the excitation energy of fission fragments and thus the number of precision neutrons. We also reanalyzed the previous data [10] by using the new level density parameters calculated by the formula proposed by Tōke and Swiatecki [13] and examined the dependence of the precision multiplicities of charged particles on the compound nucleus fissility.

II. EXPERIMENTAL METHOD

The compound nucleus ^{178}W was produced in the $^{19}\text{F} + ^{159}\text{Tb}$ reaction using ^{19}F beams from the JAERI tandem accelerator. A self-supporting ^{159}Tb target of 1.03 mg/cm² thickness was used, and the bombarding energy was varied from 124.1 to 159.1 MeV to obtain the excitation function of charged particle multiplicity. Protons and α particles were measured by six ΔE - E counter telescopes. Each counter telescope consists of a thin silicon surface barrier detector (ΔE) of 30 μm thickness and a thick silicon surface barrier detector (E) of 2000 μm thickness. These counter telescopes were placed at the backward angles $\theta = 110^\circ$ and 145° with respect to the beam direction. This is because charged particles mea-

sured at the backward angles are predominantly those evaporated statistically from the excited nucleus ^{178}W . In order to measure the out-of-plane angular distributions of charged particles, four counter telescopes at $\theta=110^\circ$ were placed at the in-plane ($\varphi_L=90^\circ$) and at the out-of-plane angles $\varphi_L=65^\circ$, 40° , and 15° and two counter telescopes at $\theta=145^\circ$ were placed at $\varphi_L=78^\circ$ and 62° . Here the out-of-plane angle is defined as the angle between the normal to the reaction plane and the particle emission directions. The solid angles of these counter telescopes were 6.8 msr. As shown in [10], emission sources of charged particles in the fission process are easily identified by placing the light particle counters perpendicular to the fission direction. Thus all light particle counters were placed on the positions perpendicular to the fission direction. Protons and α particles were measured in coincidence with both fission fragments. The energies of protons and α particles were calibrated by using the α particle energy of 5.486 MeV from an ^{241}Am source and a precision pulser.

Both fission fragments were measured in kinematical coincidence with each other by a silicon surface barrier detector of $60\ \mu\text{m}$ thickness with a large solid angle ($\Omega=58\ \text{msr}$) and a position sensitive avalanche detector ($10\ \text{cm}\times 10\ \text{cm}$) with the opening angle of 22° . The silicon surface barrier detector was placed at $\theta=-115^\circ$, and the position sensitive avalanche counter was placed at $\theta=37^\circ-40^\circ$ depending on the bombarding energy. The negative sign in angle means the opposite side of the $\Delta E-E$ counter telescopes with respect to the beam direction. The position sensitive avalanche counter consists of two sets (corresponding to X and Y position measurements) of a parallel-plate avalanche counter; each consists of an aluminized thin polyester foil ($70\ \mu\text{g}/\text{cm}^2$) and a wire frame on which gold plated tungsten wires ($10\ \mu\text{m}$ diameter) are stretched at intervals of 2 mm. The angle resolution of this detector was 0.2° .

The folding angle between the emission directions of both fission fragments was measured to confirm the complete momentum transfer fusion followed by fission at

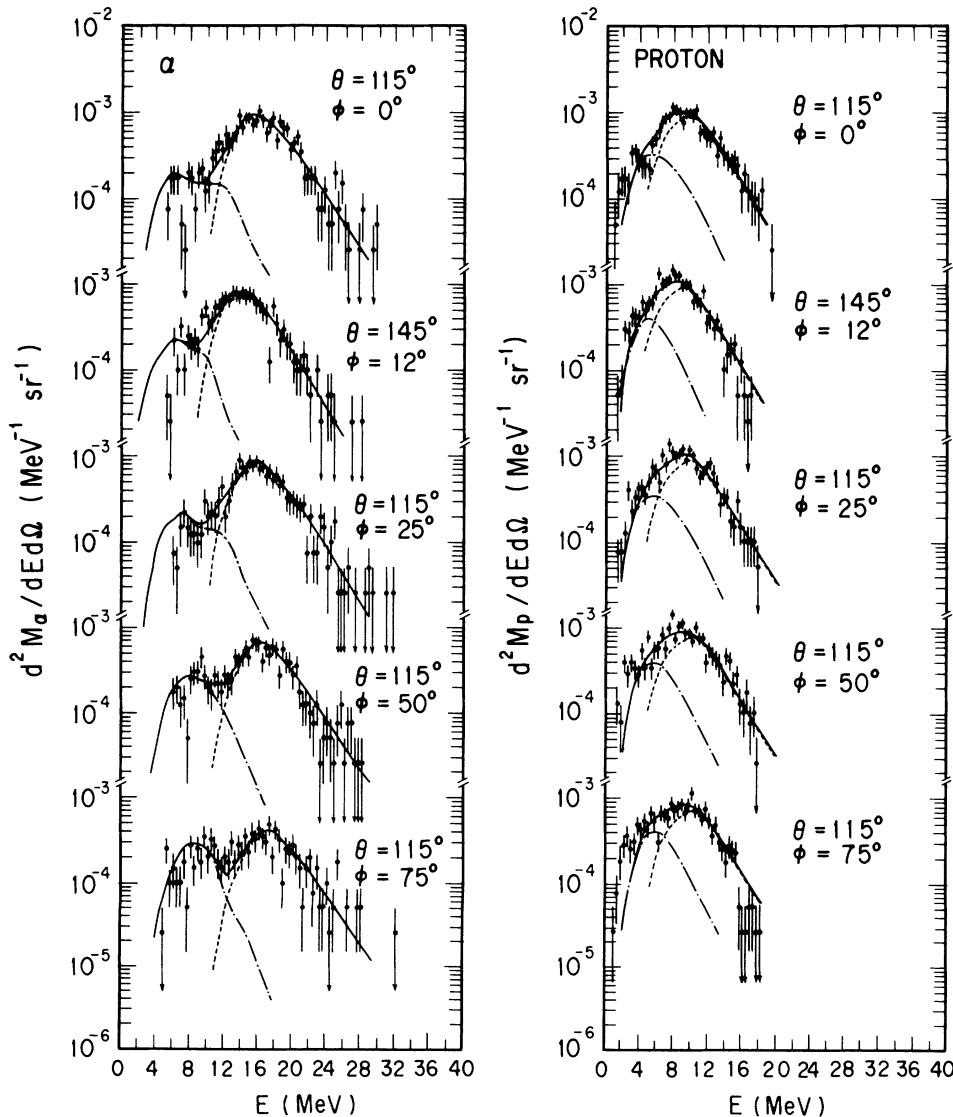


FIG. 1. Typical energy spectra of protons and α particles measured in coincidence with fission fragments in the $^{19}\text{F}+^{159}\text{Tb}$ reactions with a bombarding energy of 159.1 MeV. The in-plane and out-of-plane angles of the charged particle counters in the laboratory system are denoted as θ and ϕ , where $\phi=90^\circ-\varphi_L$ (see text). The calculated energy spectra of protons and α particles emitted from the compound nucleus (CE) and fission fragments (FE) are shown as the dashed and dot-dashed lines, respectively. The sums of the two components are shown as the solid lines.

each bombarding energy. All measured folding angles agreed with the predicted angles by assuming the complete momentum transfer within the experimental error.

III. EXPERIMENTAL RESULTS

Typical energy spectra of protons and α particles measured in coincidence with fission fragments are shown in Fig. 1. The ordinate is a differential multiplicity of an emitted particle,

$$\frac{d^2M}{dE_p d\Omega_p} = \left(\frac{d^3\sigma_{\text{coin}}}{dE_p d\Omega_f d\Omega_p} \right) / \left(\frac{d\sigma_f}{d\Omega_f} \right),$$

where $d\sigma_f/d\Omega_f$ is the differential cross section of the fission fragments at the angle where the fission fragments were measured in the coincidence measurements and E_p and Ω_p the laboratory energy and the solid angle of a charged particle, respectively. The low energy threshold of about 5 MeV in the α particle spectra comes from the maximum energy of α particles which stop in the ΔE detectors and consequently the particle identification was impossible below this energy. The high energy threshold of about 17 MeV in the proton spectra comes from the minimum energy of protons which pass through the E detectors, because of the insufficient thickness of the E counters to stop high energy protons.

Each coincidence energy spectrum consists of two main components, that is, the component (CE) emitted from the compound nucleus prior to fission and the one (FE) emitted from fully accelerated fission fragments. The low energy peaks observed in the α particle spectra correspond to the FE and the high energy peaks correspond to the CE. These CE and FE components are not clearly separated in the proton energy spectra, because the emission barrier heights for protons from the compounds nucleus and those from the fission fragments are not sufficiently enough different from each other. The near scission emission component, which has been observed in fission of heavy compound nuclei [11,14], was not evident in the present reactions.

In order to obtain the multiplicities of the CE and FE components, the measured spectra were fitted by the CE and FE spectra calculated by the statistical model using the code PACE2 [15]. Since the calculations and fitting procedure are the same as those written in [10], only important points for the present analysis are shown here. The observed CE components were fitted by the calculations in which the particle emission barrier heights were reduced by the amount of 2.0 MeV for α particles and 1.25 MeV for protons from the optical-model potentials of Huizenga and Iga [16] and Perey and Perey [17], respectively. As shown in [10], the FE components were calculated by reducing the particle emission barrier heights by the amount of 0.5 MeV for α particles and 0.25 MeV for protons from these optical-model potentials. Absolute values of the calculated CE spectra were normalized to the observed CE components at each angle. The calculated FE spectra, which were the sum of emissions from two fission fragments, were fitted by adjusting a normalization constant to the observed FE com-

ponents at all angles. The calculated spectra fitted to the observed spectra are shown in Fig. 1 as dashed lines for the CE and dot-dashed lines for the FE. The sum of the two components is shown as solid lines. The proton and α particle spectra measured at several in-plane and out-of-plane angles are well reproduced by the calculated spectra.

The CE and FE components thus obtained were integrated in energy at each angle. The CE components are shown in Fig. 2 as a function of the out-of-plane angle φ which is defined in the center-of-mass system. The out-of-plane angular distributions were fitted by the function

$$W(\varphi) = W_0 \exp(\beta_2 \sin^2 \varphi),$$

where β_2 and W_0 are fitting parameters. The precession multiplicities for protons and α particles were obtained

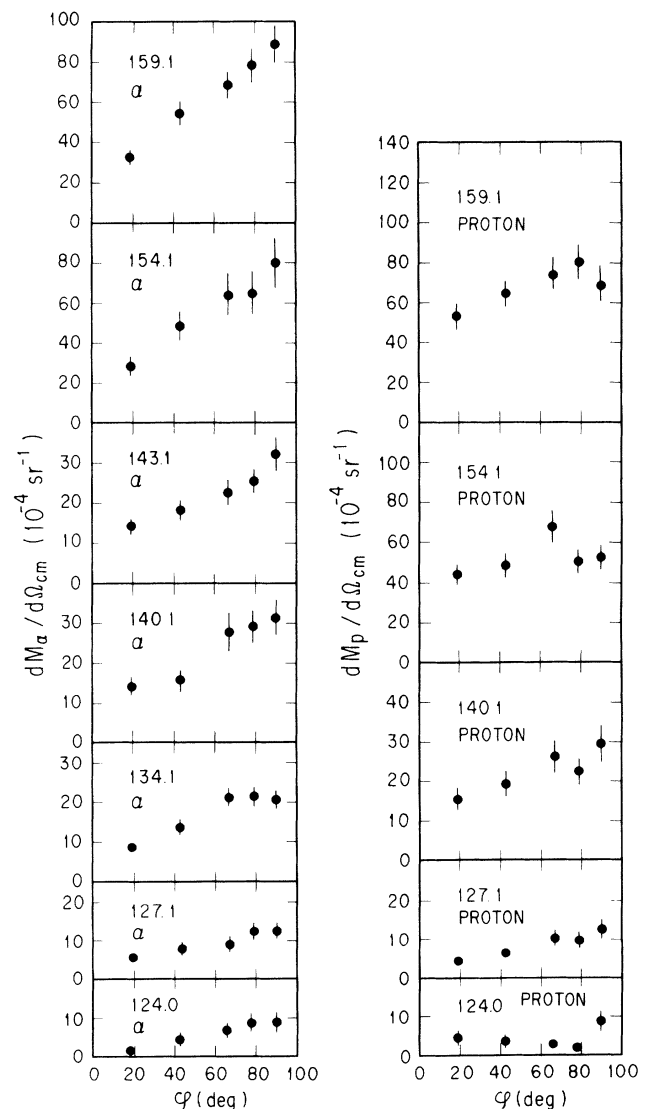


FIG. 2. Out-of-plane angular distributions of precession protons and α particles measured in the $^{19}\text{F} + ^{159}\text{Tb}$ reactions. The laboratory bombarding energies are shown for each angular distribution. φ is the out-of-plane angle defined in the center-of-mass system.

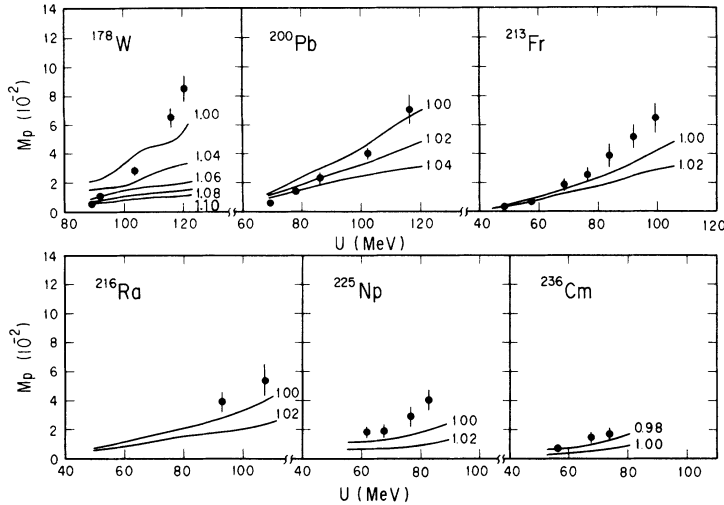


FIG. 3. Precession proton multiplicities as a function of the compound nucleus excitation energy U . The types of the compound nuclei are shown. The solid lines represent the statistical-model calculations, where the various values of the ratio of a_f/a_n as shown in the figure were assumed.

by integrating the out-of-plane angular distributions of the CE. The energy integrated FE components were found to be rather isotropic in the rest frame of the fission fragment. The postscission multiplicities for protons and α particles were obtained by multiplying the energy integrated FE components by 4π .

IV. DISCUSSION

A. Precession multiplicities

Measured precession multiplicities M_p for protons and M_α for α particles are plotted as a function of the compound nucleus excitation energy U in Figs. 3 and 4, together with the data obtained for the heavier compound nuclei [10]. The definition of U is the same as those written in [10]. These data were compared to the statistical-model calculations. Emissions of neutrons, protons, α particles, and γ rays from excited nucleus and the fission competition were taken into account using the statistical-model code PACE2. The transmission coefficients for neutron, proton, and α particle emissions were calculated using the optical-model potential of [16] and [17]. The modified emission barrier heights for pro-

tons and α particles discussed in Sec. III were used in the present calculations. The emission barrier heights for protons and α particles from the heavier systems are given in [10].

The level density parameter a_n was estimated using the formula proposed by Töke and Swiatecki [13]. The ratio a_f/a_n of the level density parameters of the saddle point deformation to the ground state deformation is a sensitive quantity to the calculated multiplicity. Although the ratio and fission barrier height B_f have been extensively studied [18–20], it is experimentally rather difficult to determine these quantities separately. This is because the two quantities are strongly correlated in the competition of the particle emission and the fission decay which determine the fission and evaporation residue cross sections and also the precession particle multiplicity. Among these, the precision neutron multiplicity is less sensitive to B_f and then Ward *et al.* [21] could determine experimentally the ratio a_f/a_n to be 1.02 ± 0.02 in the $^{19}\text{F} + ^{181}\text{Ta}$ reaction. Töke and Swiatecki proposed the formula to calculate the level density parameter by taking into account the surface diffuseness of nuclear density distribution. Their calculations show that the ratio

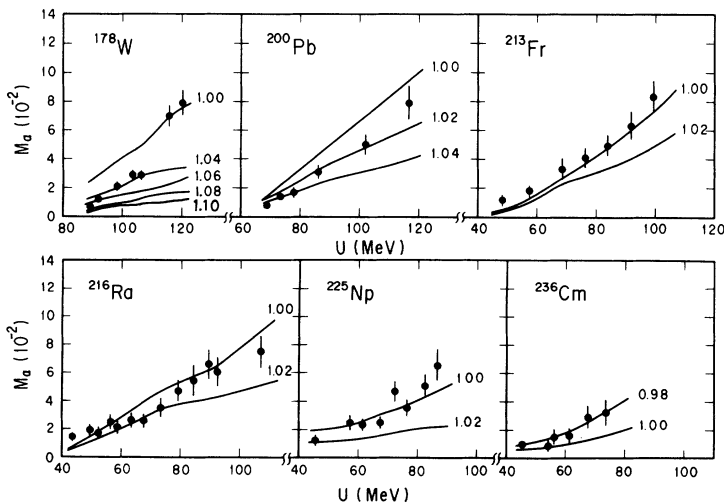


FIG. 4. Same as Fig. 3, but for the precision α particle multiplicities.

a_f/a_n is normally greater than unity and approaches to unity when nucleus becomes heavy, that is, $(a_f/a_n)_{\text{cal}}=1.13$ for ^{178}W and 1.03 for ^{236}Cm .

The calculated results assuming various values of a_f/a_n are shown in Figs. 3 and 4 as solid lines. Here the fission barrier heights were estimated as $B_f=kB_{\text{RFRM}}$, where B_{RFRM} is a value calculated by the rotating finite range model [22] and k an adjustable parameter to reproduce the observed fission and evaporation-residue cross sections. The parameters k for the heavy nuclei except ^{178}W are shown in [10] together with the diffuseness parameter of the entrance channel angular momentum. In the case of ^{178}W , k were varied from 0.92 to 1.27 depending on the value of a_f/a_n of 1.00–1.10 to reproduce the observed fission and evaporation-residue cross sections of [23]. The diffuseness parameter of the entrance channel angular momentum was fixed to $4.2\hbar$.

1. Nucleus ^{178}W

The precission multiplicities of protons and α particles measured at the low excitation energy $U \approx 90$ MeV are well reproduced by the calculation with $a_f/a_n=1.08$ –1.10, while these calculations fail to reproduce the high energy data measured at $U \approx 120$ MeV. On the other hand, the calculation with $a_f/a_n=1.00$, which agrees with the data at $U \approx 120$ MeV, overestimates considerably the multiplicity at the low excitation energy. If the value of a_f/a_n decreases from 1.10 to 1.00 as U increases, the observed multiplicities would be reproduced by the statistical-model calculation. This is, in principle, possible. Since the angular momentum L contributing to fission increases as U , the saddle point shape becomes more compact than the one with $L=0$. This makes the correction for a_f smaller at large L due to the decrease of the surface area [13]. Therefore the value a_f/a_n decreases towards unity as U increases. Using the saddle point shape calculated by the rotating liquid drop model [12] and also the prescription of Bishop *et al.* [24], the ratio a_f/a_n in the case of ^{178}W decreases slowly as L increases up to $78\hbar$ and then rapidly comes close to unity near $L=81\hbar$, where the fission barrier vanishes. On the

other hand, the present statistical-model calculation shows that the average angular momentum contributing to the precission particle emission slightly increases from $61\hbar$ to $65\hbar$ as U increases from 90 to 120 MeV. This means that the ratio a_f/a_n is almost constant in the present excitation energy region ($U=90$ –120 MeV).

After the compound nucleus is formed, the fission width at the saddle point increases from zero to an equilibrium value. This transient time during which the fission width reaches to the equilibrium value at the saddle point is called presaddle delay time. In the present work, we distinguish the presaddle delay time from the fission delay time, which is defined as the sum of the presaddle delay time and a saddle-to-scission time. Since the fission probability is still small during the presaddle delay time, emissions of neutrons, protons, and α particles are enhanced and become important at the high excitation energies where the particle decay time (essentially equal to the neutron decay time \hbar/Γ_n for the present heavy nuclei) becomes comparable to the presaddle delay time τ . Consequently, the statistical-model calculation without taking into account the presaddle delay time may fail to predict the multiplicities at high excitation energies. It was found that from the precission neutron measurement the fission dynamics becomes relatively important at $U \geq 90$ MeV in the the $^{20}\text{Ne}+^{150}\text{Nd}$ reaction [2], where the compound nucleus ^{170}Yb close to the present reaction system is formed. This means that the statistical-model calculation without the presaddle delay time is valid below 90 MeV, indicating that the values 1.08–1.10 for the ratio a_f/a_n are adequate in the ^{178}W case. These values are also consistent with the experimental result ($a_f/a_n=1.03_{-0.03}^{+0.07}$) obtained in the $^{141}\text{Pr}+^{35}\text{Cl}$ reaction [18] (compound nucleus ^{176}Os). In the present calculations we adopted $a_f/a_n=1.08$ –1.10.

As shown in Figs. 3 and 4, the calculations with $a_f/a_n=1.08$ –1.10 underestimate considerably the precission multiplicities for both protons and also α particles at $U \geq 100$ MeV. We can extract the presaddle delay time from the present data by assuming the whole observed excess multiplicities over the calculated ones are caused by the suppression of the fission probability at an

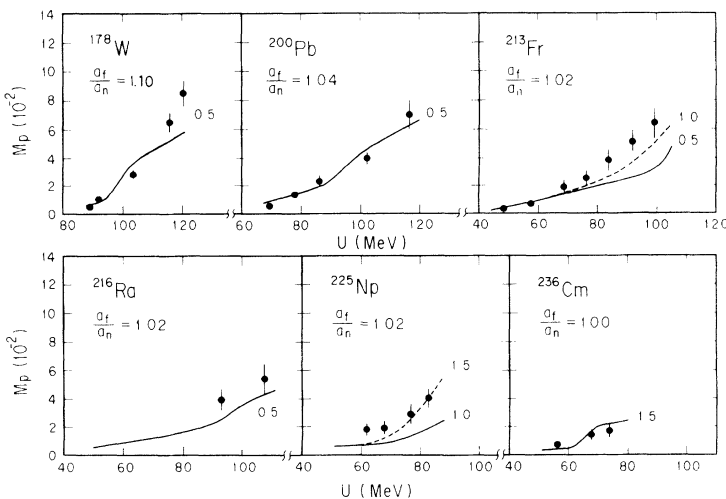


FIG. 5. Same as Fig. 3, but the calculated precission proton multiplicities with taking into account the various presaddle delay times (unit of 10^{-20} sec) are shown as the solid and dashed lines.

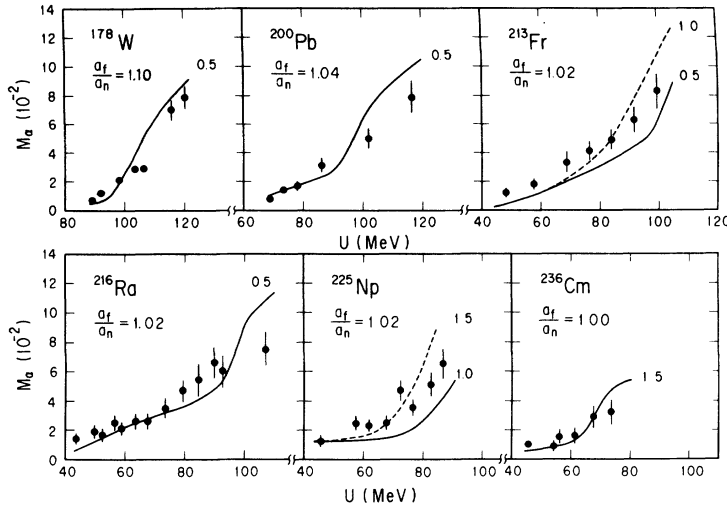


FIG. 6. Same as Fig. 5, but for the calculated precession α particle multiplicities.

initial stage of the fission process. For this purpose, the statistical model code PACE2 was modified so as to include the presaddle delay time τ . The fission decay width was taken to be zero up to time τ and the full statistical-model value for longer times (sharp cutoff approximation), and only neutrons, protons, α particles, and γ rays were considered as allowed decay modes during this time period.

The calculated results with $\tau=0.5 \times 10^{-20}$ sec are shown in Fig. 5 for protons and Fig. 6 for α particles, where $a_f/a_n=1.10$ was assumed. The calculated multiplicities increase rapidly at $U \geq 90$ MeV. By increasing τ more than 0.5×10^{-20} sec, the calculated proton multiplicity comes close to the data $U=120$ MeV, while the calculations for the α particle multiplicity overestimate at $U=120$ MeV. The calculations with $a_f/a_n=1.08$ give almost the same result as those with $a_f/a_n=1.10$. As shown in Figs. 3 and 4, the suppression of the fission probability gives rise to an enormous enhancement of M_p and M_α in the present reaction system. This is a characteristic feature observed in the ^{178}W . On the other hand, the enhancement of charged particle emissions due to the suppression of the fission probability is smaller for heavier compound nuclei as shown later.

The present analysis for the ^{178}W shows that the presaddle delay time of around 0.5×10^{-20} sec is needed to reproduce the observed precession multiplicities of protons and α particles. The calculated precession neutron multiplicities with $\tau=0$ and 0.5×10^{-20} sec and $a_f/a_n=1.10$ were compared to the data measured by Newton *et al.* [25] in the same reaction system as the present case. As shown in Fig. 7(c), the calculated results considerably underestimate the data. This inconsistency is a common feature observed in comparison of the precession neutron data and charged particle data. As pointed out by Lestone *et al.* [11] and also in [10], precession charged particles, especially α particles, are predominantly emitted before saddle. This is consistent with the statistical-model prediction, which shows that the most of charged particles tend to be emitted at the first chance without preceding neutron emissions and are unlikely to be emitted from the states with low excitation energies

after several neutrons are emitted. On the other hand, the precession neutrons which are the dominant decay mode can be emitted throughout the whole fission path, and thus a saddle-to-scission time in addition to the presaddle delay time is needed to account for the precession neutron data.

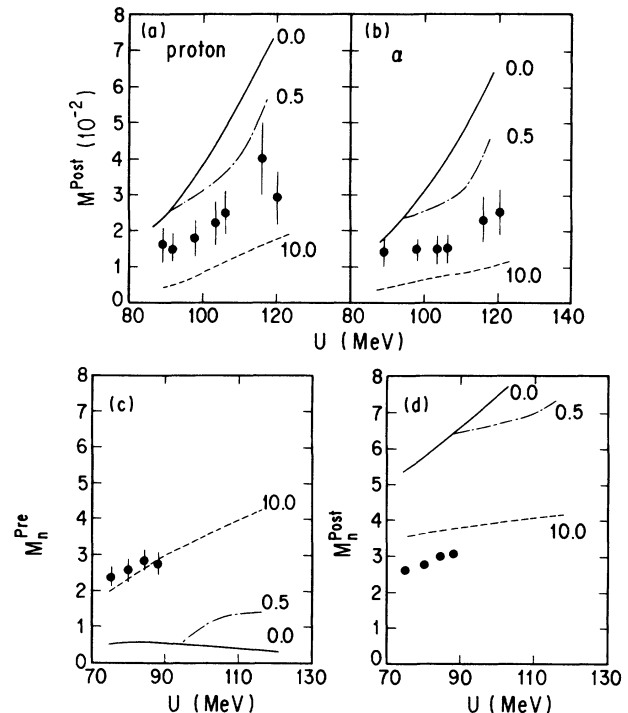


FIG. 7. (a), (b) Postscission proton and α particle multiplicities in the $^{19}\text{F}+^{159}\text{Tb}$ reactions as a function of the compound nucleus excitation energy U . The calculated results with and without taking into account the presaddle delay time τ are shown as the dot-dashed lines ($\tau=0.5 \times 10^{-20}$ sec), the dashed lines ($\tau=10.0 \times 10^{-20}$ sec), and the solid lines ($\tau=0$). Here the ratio $a_f/a_n=1.10$ was assumed. (c), (d) Precession and postscission neutron multiplicities in the $^{19}\text{F}+^{159}\text{Tb}$ reactions measured by Newton *et al.* [25] are shown as a function of U . The calculated results with various values of τ are shown.

2. Nuclei ^{200}Pb , ^{213}Fr , ^{216}Ra , ^{225}Np , and ^{236}Cm

We previously reported the measurements of the pre-scission multiplicities for protons and α particles from the compound nuclei ^{200}Pb , ^{213}Fr , ^{216}Ra , ^{225}Np , and ^{236}Cm [10]. It is worthy to compare those data with the present data in order to clarify the dependence of pre-scission charged particle multiplicities on the fissility of nucleus. The level density parameters were estimated by the formula of [13] instead of $a = A/10$, which was used previously. The new value was $A/8.5$ for the ^{200}Pb . This modification caused about 30% reductions of the calculated multiplicity.

The statistical-model calculations without the presaddle delay time are shown in Figs. 3 and 4 as solid lines. The ratio a_f/a_n of 1.02 ± 0.02 , which is the experimental value obtained by Ward *et al.* [21], was used for the ^{200}Pb , and for the other nuclei the ratio was varied around unity. The calculated results are the same as those previously reported except for the overall reduction of about 30%. Although the calculated results fairly agree with the observed data for all compound nuclei studied, a small discrepancy with the data exists. For instance, the calculation with $a_f/a_n = 1.02$ in the ^{200}Pb agrees with the α particle data well, but the agreement with the proton data is worse. If $a_f/a_n = 1.04$ is assumed, the agreement with the low energy data becomes better, but the calculation underestimates the multiplicities of protons and α particles at high excitation energies. This is the similar situation we met in the nucleus ^{178}W , but the extent of the disagreement is smaller for the ^{200}Pb . The calculations including the presaddle delay time of 0.5×10^{-20} sec are shown in Figs. 5 and 6, where $a_f/a_n = 1.04$ is assumed. The agreement with the data for the ^{200}Pb becomes better. Thus the data for the ^{200}Pb are equally well reproduced by the calculations with $a_f/a_n = 1.02$ and $\tau = 0$ and also the calculations with $a_f/a_n = 1.04$ and $\tau = 0.5 \times 10^{-20}$ sec. This means that the presaddle delay time of around 0.5×10^{-20} sec is not inconsistent with the data for the ^{200}Pb .

The observed multiplicities for α particles from the nuclei ^{213}Fr , ^{216}Ra , ^{225}Np , and ^{236}Cm are well reproduced by the calculations without any presaddle delay time as shown in Fig. 4. There is no definite evidence for the enhancement of the observed multiplicities over the statistical-model calculations, where $a_f/a_n = 1.00$ was assumed for the nuclei ^{213}Fr , ^{216}Ra , and ^{225}Np and $a_f/a_n = 0.98$ for the ^{236}Cm . On the other hand, the same calculations always somewhat underestimate the observed multiplicities for protons at high excitation energies as shown in Fig. 3. The low energy proton data at $U \sim 50$ MeV for the ^{213}Fr , for instance, are reproduced by the calculation with $a_f/a_n = 1.02$ as well as those with $a_f/a_n = 1.00$, but the high energy data are always larger than both calculated results. Some enhancements at high excitation energies also exist in the proton data for ^{216}Ra , ^{225}Np and ^{236}Cm . If these enhancement are caused by the suppression of the fission probability during the presaddle delay time, the upper limit of the presaddle delay time could be estimated from the present data. In order to deduce the upper limit, we assumed $a_f/a_n = 1.02$ for

^{213}Fr , ^{216}Ra , and ^{225}Np and $a_f/a_n = 1.00$ for ^{236}Cm . The calculated results with the various presaddle delay times are shown in Fig. 5 for protons, and for reference, the calculated results for α particles are shown in Fig. 6. The upper limit of the presaddle delay time was around $(0.5 - 1.5) \times 10^{-20}$ sec.

It is noted that the estimated upper limit strongly depends on the value of the ratio a_f/a_n . The ratio should be determined so as to reproduce the data measured at the low excitation energy where the fission delay time is negligible compared to the statistical model value of the fission decay time (\hbar/Γ_f). The number of the data points at low energy proton data is not sufficient to determine the value of the ratio. Thus the deduced value for the upper limit reflects greatly the uncertainty of the ratio a_f/a_n .

B. Post scission multiplicities

Measured postscission multiplicities of protons and α particles are plotted in Figs. 7(a) and 7(b), respectively. These multiplicities increase slowly as a function of U in contrast with the pre-scission charged particle multiplicities shown in Figs. 3 and 4. Since the postscission particle multiplicities strongly depend on the excitation energy of fission fragments, the present result indicates that the excitation energies of fission fragments also increase slowly as U . This energy dependence is similar to that of the postscission neutron multiplicity measured by Newton *et al.* [25] in the same reaction system as the present one. A slow increase of the pre-scission neutron multiplicity which are plotted in Fig. 7(d) indicates that the excitation energies of fission fragments are almost constant.

In order to investigate the effect of the fission delay time on the postscission particle multiplicities, the evaporations of neutrons, protons, and α particles from excited fission fragments were calculated by estimating the fragment excitation energy individually from the statistical-model calculation and the measured pre-scission neutron multiplicity. The excitation energies E_1 and E_2 of fission fragments were estimated by using the excitation energy U_d of the final daughter nuclei just before fission and the total kinetic energy E_{TKE} predicted by Viola, Kwiatkowski, and Walker [26] as follows:

$$E_1 + E_2 = U_d + Q - E_{\text{TKE}},$$

$$Q = M_d - M_1 - M_2,$$

where M_d , M_1 , and M_2 are the mass excesses of the daughter nucleus and two fission fragments. In general, the excitation energy U_d is distributed reflecting the number of the pre-scission neutrons. This energy distribution of U_d was taken into account in the present calculation. The neutron to proton ratio N/Z of fission fragment was assumed to be the same as the daughter nucleus just before fission. Although the particle evaporations from the symmetric mass fragments were, for simplicity, calculated ($M_1 = M_2$) at all excitation energy U , the calculations taking into account the fragment mass distribution were also performed at the two energies of $U = 89$ and 121.2 MeV. In this case the fragment mass distribu-

tions were estimated from those measured in the $^{32}\text{S}+^{144}\text{Sm}$ reactions [27], which produce the compound nucleus ^{176}Os close to the present compound nucleus ^{178}W . The calculations taking into account the realistic fragment mass distributions gave the same results within about 10% as those calculated for the symmetric mass fragments.

The calculated results without taking into account the fission delay time are shown as solid lines in Figs. 7(a) and 7(b). The calculations considerably overestimate the postscission multiplicities of protons and α particles at $U > 100$ MeV. This is because the calculated pre-scission neutron multiplicities (solid line) are considerably smaller than the observed values as shown in Fig. 7(c), and thus the excitation energies of fission fragments are overestimated. Since the number of the pre-scission neutrons mainly limits the fragment excitation energy, the energy can be determined by the calculation which reproduces the pre-scission neutron multiplicity data. For this purpose, the presaddle delay time was adjusted as a parameter to reproduce the pre-scission neutron data. The large presaddle delay time of $\tau = 10 \times 10^{-20}$ sec was needed to get a good fit to the observed pre-scission neutron data [see Fig. 7(c)]. This absolute value should be understood as an effective value which include the saddle-to-scission time. The calculated results underestimate the postscission multiplicities of protons and α particles, while the postscission neutron multiplicities slightly overestimated as shown in Fig. 7(d). This fact suggests that an average fragment excitation energy for emissions of charged particles is larger than the one for emission of neutrons. The reason of this is not clear. In the present calculations, the fragment excitation energy distribution was estimated by calculating the excitation energy distribution of the final daughter nucleus just before fission. However, it is not verified that the present calculation simulates properly the true distribution of the pre-scission neutrons, because only the average number of the pre-scission neutrons as the measured pre-scission neutron multiplicity is reproduced by the present calculation, but the distribution itself is unknown. The distribution of the fragment excitation energy is likely to account for this inconsistency.

The calculated results assuming $\tau = 0.5 \times 10^{-20}$ sec are shown as dot-dashed lines. These calculations overestimate the postscission multiplicities of protons and α particles, because the calculated pre-scission neutron multiplicity is too small and thus the fragment excitation energy is not properly estimated. This fact means that the time scale probed by pre-scission charged particles and the one probed by pre-scission neutrons are clearly different and the later is longer than the former. The present postscission charged particle data show that the fission fragments are colder than the predictions without

taking into account the fission delay time and slightly hotter than the value estimated from the pre-scission neutron data. This fact, together with the short presaddle delay time of around 0.5×10^{-20} sec, suggests that the saddle-to-scission time is so long that a fairly large amount of the pre-scission neutrons are emitted even for the light compound nucleus ^{178}W whose saddle-to-scission path length is expected to be short as shown in [25].

V. SUMMARY AND CONCLUSIONS

The pre-scission and postscission multiplicities of protons and α particles were measured in the $^{19}\text{F}+^{159}\text{Tb}$ reactions. The observed pre-scission multiplicities of protons and α particles were enhanced compared to statistical-model calculations, and the presaddle delay time of around 0.5×10^{-20} sec was needed to reproduce both pre-scission charged particle multiplicities. On the other hand, this value was too small to account for the pre-scission and postscission neutron multiplicities measured by Newton *et al.* [25], implying that a part of the pre-scission neutrons is emitted from the saddle-to-scission region. The pre-scission multiplicities of protons and α particles previously measured in the heavy compound nuclei ^{200}Pb , ^{213}Fr , ^{216}Ra , ^{225}Np , and ^{236}Cm [10] were reanalyzed by using the level density parameters proposed by Töke and Swiatecki. The data of protons and α particles in the ^{200}Pb were consistent with the calculations with taking into account the presaddle delay time of around 0.5×10^{-20} sec. Although the data for the nuclei ^{231}Fr , ^{216}Ra , ^{225}Np , and ^{236}Cm were consistent with the statistical-model calculations without taking into account the presaddle delay time, the present analysis gave the upper limit of around $(0.5-1.5) \times 10^{-20}$ sec for the presaddle delay time. The measured postscission multiplicities of protons and α particles indicate that fission fragments are colder than the prediction without taking into account the fission delay time, but slightly hotter than the estimation from the observed pre-scission neutron multiplicity. From the present measurements, we conclude that in the light compound nucleus ^{178}W , the suppression of the fission probability at the initial stage of the fission process affects very sensitively to the emission probabilities of the pre-scission protons and α particles and the presaddle delay of around 0.5×10^{-2} sec is needed to reproduce the observed pre-scission multiplicities of protons and α particles. This delay time is too short to account for the pre-scission and postscission neutron multiplicity data, suggesting a long saddle-to-scission time even for the light nucleus ^{178}W whose saddle-to-scission path is expected to be short.

- [1] D. J. Hinde, D. Hilscher, H. Rossner, B. Gebauer, M. Lehmann, and M. Wilpert, *Phys. Rev. C* **45**, 1229 (1992).
 [2] D. J. Hinde, R. J. Charity, G. S. Foote, J. R. Leigh, J. O. Newton, S. Ogaza, and A. Chatterjee, *Nucl. Phys. A* **452**, 550 (1986).

- [3] W. P. Zank, D. Hilscher, G. Ingold, U. Jahnke, M. Lehmann, and H. Rossner, *Phys. Rev. C* **33**, 519 (1986).
 [4] A. Gavron, A. Gayer, J. Boissevain, H. C. Britt, J. C. Awes, J. R. Beene, B. Cheynis, D. Drain, R. L. Ferguson, F. E. Obenshain, F. Plasil, G. R. Young, G. A. Pettit, and

- C. Butler, *Phys. Rev. C* **35**, 579 (1987).
- [5] D. Hischer, H. Rossner, B. Cramer, B. Gebauer, U. Jahnke, M. Lehmann, E. Schwinn, M. Wilpert, Th. Wilspert, H. Frobeen, E. Mordhorst, and W. Scobel, *Phys. Rev. Lett.* **62**, 1099 (1989).
- [6] D. J. Hinde, H. Ogata, M. Tanaka, T. Shimoda, N. Takahashi, A. Shinohara, S. Wakamatsu, K. Katori, and H. Okamura, *Phys. Rev. C* **39**, 2268 (1989).
- [7] M. Strecker, R. Wien, P. Plischke, and W. Scobel, *Phys. Rev. C* **41**, 2172 (1990).
- [8] E. Mordhorst, M. Strecker, H. Frobeen, M. Gasthuber, W. Scobel, B. Gebauer, D. Hilscher, M. Lehmann, H. Rossner, and Th. Wilpert, *Phys. Rev. C* **43**, 716 (1991).
- [9] R. Butsch, D. J. Hofman, C. P. Montoya, P. Paul, and M. Thoennessen, *Phys. Rev. C* **44**, 1515 (1991).
- [10] H. Ikezoe, N. Shikazono, Y. Nagame, Y. Sugiyama, Y. Tomita, K. Ideno, I. Nishinaka, B. J. Qi, H. J. Kim, A. Iwamoto, and T. Ohtsuki, *Phys. Rev. C* **46**, 1922 (1992).
- [11] J. P. Lestone, J. R. Leigh, J. O. Newton, D. J. Hinde, J. X. Wei, J. X. Chen, S. Elström, and D. G. Popescu, *Phys. Rev. Lett.* **67**, 1078 (1991); J. P. Lestone, J. R. Leigh, J. O. Newton, D. J. Hinde, J. X. Wei, J. X. Chen, S. Elström, and M. Zielinska-Pfabé, *Nucl. Phys.* **A559**, 277 (1993).
- [12] S. Cohen, F. Plasil, and W. J. Swiatecki, *Ann. Phys. (N.Y.)* **82**, 557 (1974).
- [13] J. Tōke and W. J. Swiatecki, *Nucl. Phys.* **A372**, 141 (1981).
- [14] H. Ikezoe, N. Shikazono, Y. Nagame, T. Ohtsuki, Y. Sugiyama, Y. Tomita, K. Ideno, I. Kanno, H. J. Kim, B. J. Qi, and A. Iwamoto, *Nucl. Phys.* **A538**, 299c (1992).
- [15] A. Gavron (revised version of the code PACE), *Phys. Rev. C* **21**, 230 (1980).
- [16] J. R. Huizenga and G. Igo, *Nucl. Phys.* **29**, 462 (1962).
- [17] C. M. Perey and F. G. Perey, *At. Data Nucl. Data Tables* **17**, 1 (1976).
- [18] M. Beckerman and M. Blann, *Phys. Rev. Lett.* **38**, 272 (1977); *Phys. Lett.* **68B**, 71 (1977); *Phys. Rev. C* **17**, 1615 (1978).
- [19] F. Plasil, R. L. Ferguson, R. L. Hahn, F. E. Obenshain, F. Pleasonton, and G. R. Young, *Phys. Rev. Lett.* **45**, 333 (1980).
- [20] J. Van der Plicht, H. C. Britt, M. M. Fowler, Z. Fraenkel, A. Gavron, J. B. Wilhelmy, F. Plasil, T. C. Awes, and G. R. Young, *Phys. Rev. C* **28**, 2022 (1983).
- [21] D. Ward, R. J. Charity, D. J. Hinde, J. R. Leigh, and J. O. Newton, *Nucl. Phys.* **A403**, 189 (1983).
- [22] M. G. Mustafa, P. A. Baisden, and H. Chandra, *Phys. Rev. C* **25**, 2524 (1982); A. J. Sierk, Los Alamos National Laboratory Report No. LANL T9, 1984.
- [23] R. J. Charity, J. R. Leigh, J. J. M. Bokhorst, A. Chatterjee, G. S. Foote, D. J. Hinde, J. O. Newton, S. Ogaza, and D. Ward, *Nucl. Phys.* **A457**, 441 (1986).
- [24] C. J. Bishop, I. Halpern, R. W. Shaw, Jr., and R. Vandebosch, *Nucl. Phys.* **A198**, 161 (1972).
- [25] J. O. Newton, D. J. Hinde, R. J. Charity, J. R. Leigh, J. J. M. Bokhorst, A. Chatterjee, G. S. Foote, and S. Ogaza, *Nucl. Phys.* **A483**, 126 (1988).
- [26] V. E. Viola, K. Kwiatkowski, and M. Walker, *Phys. Rev. C* **31**, 1550 (1985).
- [27] B. G. Glagola, B. B. Back, and R. R. Betts, *Phys. Rev. C* **29**, 486 (1984).